Cement and Concrete Research 61–62 (2014) 1–10

Contents lists available at ScienceDirect

Cement and Concrete Research

journal homepage: http://ees.elsevier.com/CEMCON/default.asp

An observation-based model for corrosion of concrete sewers under aggressive conditions

T. Wells *, R.E. Melchers

Centre for Infrastructure Performance and Reliability, School of Engineering, The University of Newcastle, Callaghan, New South Wales 2308, Australia

ARTICLE INFO

Article history:
Received 16 June 2013
Accepted 28 March 2014
Available online 21 April 2014

Keywords:
A reaction
C corrosion
E concrete
E modeling
Other sewer

ABSTRACT

Development of rational mathematical models for prediction of the likely present and future internal corrosion of reinforced concrete sewers requires understanding of the important physico-chemical processes, preferably based on field evidence. Samples of new and 70 year old pre-corroded concretes were exposed for up to 31 months in an aggressive sewer environment at 26 °C, 98% relative humidity and 79 ppm H_2S concentration (averages). During the initial months of exposure the pH of the new concrete surfaces reduced rapidly however little corrosion loss was observed during this period. Subsequently pH reduced further, mass loss commenced and new concrete losses reached around 24 mm after 2 years. During the same period the old concrete corroded at an approximately constant rate. The presence of the corrosion product layer had negligible influence on corrosion losses. A bilinear corrosion loss model is proposed for practical applications.

1. Introduction

The safe and economic operation of existing reinforced concrete sewer systems is an issue for many wastewater operators worldwide. This requires prediction of the remaining years of satisfactory service likely to be achieved under operational conditions without premature structural failure. The issue is particularly critical for older sewers. The traditional approach to assessing the existing condition of a sewer uses visual inspection of the interior but this is expensive, disruptive and known to be not particularly accurate. Future sewer life however may be estimated from successive visual inspections using simple rules such as linear extrapolation but the confidence usually is low and data scarce [1].

It would be more useful to industry if the existing condition of a sewer could be predicted from information about its operational conditions and its material properties. In principle this also would permit extrapolation into the future and thus allow prediction of the remaining life. Such predictions require both information about operational conditions and a model to convert this information into estimates for concrete sewer corrosion. Consistent with applications in other spheres the use of models mathematically capturing accumulated knowledge and expertise from a range of other sources should permit extrapolation from data with considerably higher accuracy than is possible from extrapolation using empirical data alone [2–4].

The aim of the present paper is to develop the form and characteristics of a corrosion model based on data and observations from an actual operational sewer. While it is acknowledged that the sewer pipe corrosion process is principally driven by biological processes it is not the intention of this study to present a detailed microbiological analysis of the corrosion process. While such work is valuable, it does not of itself, advance our quantitative understanding of how the corrosion process progresses over time. The approach taken in this study is to observe the course of the sewer pipe corrosion process over time, relate it to existing theories of sewer pipe corrosion and provide models based on science subsequently simplified for practical application.

This paper is organized as follows. The next section gives an outline of the present state of knowledge of the various processes involved in concrete sewer corrosion. As noted, some of this is based on observations in actual sewers but mostly it has been obtained from laboratory experiments designed, in theory, to mimic conditions in real sewers. However in common with other long-term deterioration studies [5–8], questions remain about the transportability of laboratory tests to actual sewers. An alternative approach is to consider corrosion under natural but aggressive conditions including temperatures higher than typical for most sewers. This will accelerate diffusion and kinetic processes. Section 2 describes the relevant test conditions and Section 3 reports the observations. This is followed by a discussion of the results, the introduction of a bilinear model for corrosion loss estimation in practical applications and conclusions.

1.1. Background

Over a century ago Olmstead and Hamlin [9] first observed the corrosion of cement mortar in an outfall sewer constructed only 5 years

* Corresponding author. Tel.: +61 2 4921 5741; fax: +61 2 4921 6991.
E-mail address: Tony.Wells@newcastle.edu.au (T. Wells).

http://dx.doi.org/10.1016/j.cemconres.2014.03.013
0008-8846/

earlier. In their report the primary corrosive agent was correctly identified as sulfuric acid which was linked to the presence of acidic gases given off during putrefaction of sewage wastes. The sulfuric acid was considered to have reacted with the mortar lining to form expansive gypsum that caused spalling and fracture of the brickwork sewer.

Biological influences became associated with sewer corrosion following the identification of the bacterium *Acidithiobacillus thiooxidans* (originally named *Thiobacillus concretivorous*) among the acidic corrosion products [10–13]. Numerous other bacterial and fungal species have since been associated with the sewer corrosion process [14–17] while a recent pyrosequencing study of corroded sewer pipe in two Australian sewers [18,19] revealed a diverse range of bacteria and fungi of which *Acidothiobacillus* spp. constituted only a minor portion.

Microbiologically influenced corrosion (MIC) was not regarded as significant for concrete sewers until the 1980s when corrosion rates increased significantly both in the USA [20] and in Europe [21]. Eventually the increase was linked to a reduction in the concentration of biologically toxic metals, such as lead, mercury and arsenic, discharged to sewers following the introduction of 'clean water' legislation such as the 1980 U.S. Clean Water Act [22]. Since these metals are toxic to microorganisms, their reduction had the unintended consequence of increased bacterial populations and activity with consequent increased MIC. In recent decades increased MIC has been also been linked to the greater discharge of sulfate containing detergents to sewers, increases in protein consumption, higher sewage temperatures as well as increased length of sewer lines (and hence sewage residence times) caused by increasing suburban areas and populations [23].

The challenges posed by the increasing influence of MIC in the 1970s and 1980s prompted an increased research effort particularly in Germany [17,24,25] and also the publication of design manuals which listed procedures for estimating corrosion rates [26,27]. More recently studies aimed at improving our understanding and quantification of the underlying mechanisms of the sewer corrosion processes [28–32] as well as the bacterial population dynamics and kinetics involved [8, 33–35] have been conducted. Much of the research has employed laboratory experimentation and has focussed on examining individual facets of the corrosion process. Despite much research progress, practical management of sewer corrosion is still hindered by a limited understanding of the in-sewer processes causing sewer corrosion and how those processes evolve with time.

Sewer corrosion processes vary over time in a complex fashion. Conditions on the exposed pipe surface change as chemical (abiotic) and biotic processes alter the surface chemistry. In turn surface conditions help determine the nature and magnitude of corrosive activities taking place. This was recognized in the three stage model first proposed by Islander et al. [36] in which concrete sewer pipe corrosion initially proceeds principally by chemical (abiotic) acidification of the pipe surface followed by MIC driven by a succession of evolving microbial communities (Fig. 1).

In brief, the model has the following features. In stage 1, the calcium hydroxide present in the concrete matrix of new concrete dissolves in the concrete pore water and any surface condensate film will have a pH of ~12 to 13 [37]. This is too alkaline for the colonisation and growth of most bacterial species. Thus biologically driven corrosion is minimal. During this time any acidic gases present in the sewer atmosphere, such as CO_2 and H_2S, dissolve in the condensate film, reacting with the alkali species thereby abiotically lowering the surface pH towards neutral levels. The abiotic oxidation of H_2S also produces thiosulfates and polythionic acids [36].

Once the surface pH falls below pH = 9, conditions become favourable for the colonisation of the surface by a number of microbiological species and the corrosion process now enters stage 2. Among the species present at this stage are neutrophilic sulfur oxidising organisms (NSOM) [8,36], nitric acid producing nitrifiers (which have been linked to the corrosion of concrete [21,38,39]), as well as fungal species [21,40] which produce a range of carboxylic acids (including acetic, oxalic and glucuronic acids) that further lower the pipe surface pH [41]. As the pH falls to near neutral, surface biological oxidation of sulfur species occurs, dominated by the oxidation of thiosulfates to polythionates and sulfates [8,36]. This lowers the surface pH even further.

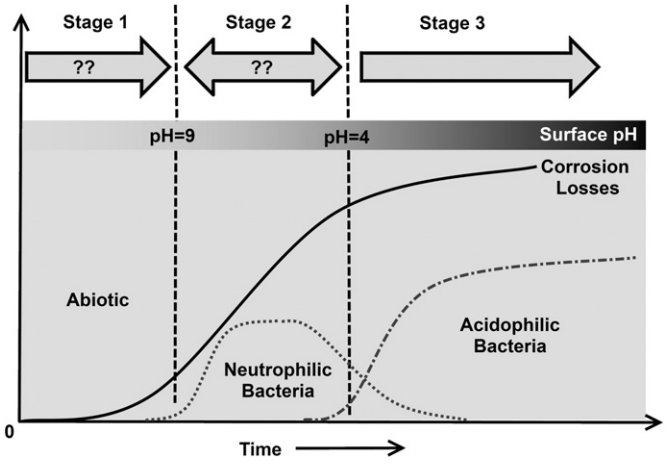

Fig. 1. The corrosion of concrete sewer pipe as a three stage process as originally proposed by Islander et al. (adapted from [36]).

When the surface pH reaches about 4 the corrosion process enters stage 3 and a significant increase occurs in the colonisation of the surface by acidophilic sulfur oxidising microorganisms (ASOM). Abiotic and biological oxidation at these conditions converts H_2S to elemental sulfur which in turn is readily oxidised to sulfates by the ASOM present. The acids produced by the ASOM and to a lesser extent the NSOM attack the alkaline components (portlandite, calcium silicates and calcium aluminates) within the cement binder to form gypsum, $CaSO_4.2H_2O$, and the mineral ettringite, $3CaO.Al_2O.3CaSO_4.32H_2O$ [40]. The accompanying increase in volume (124% and 227% respectively) [42] causes formation of cracks and internal voids, reducing the structural integrity of the pipe wall and facilitating permeation of moisture, acids and biota into the concrete structure, thereby propagating the corrosion cycle.

As noted by Roberts et al. [43] little quantitative assessment of the Islander model as a whole has been undertaken as recent MIC research has focused on sewer pipe in advanced stages of corrosion (for example [1,16,44,45]). In order to predict the service life of a concrete sewer pipe a better quantitative picture of the overall process is needed, however only a limited number of studies have examined the initial stages of sewer pipe corrosion [43] or the overall process [8].

As part of a larger study [46], the opportunity arose to use a working sewer main with particularly aggressive internal environmental conditions to examine the relationship between the corrosion of samples of realistic concretes (both new and previously corroded 70 year old sewer pipe) and the internal sewer environment. As described below, this permitted direct observation of the results of the corrosion process at different time intervals. It also allowed construction of a corrosion loss curve for the concrete sewer under the specific in-situ conditions and a quantitative rendering of the three stage model proposed by Islander et al. [36]. This information will be significant in the eventual development of a mathematical model.

2. Experimental design

2.1. Materials

Two different concretes were exposed in the sewer. The 'new' coupons were cut from newly manufactured 1.2 m ID spun cast standard reinforced concrete sewer pipe. The 'old' coupons were cut from reinforced concrete that had served for 70 years as covers for a typical operating sewer carrying domestic, industrial and trade waste. The original

covers had corroded considerably leaving 80 to 100 mm remaining thickness. The old coupons retained a ~2 mm thick crystalline layer of corroded material generated during the earlier 70 years of exposure to the sewer environment. The concretes were cut to 100 mm (nominal) cubes. Care was taken to ensure that the previously corroded face of the old coupons was left undisturbed during cutting and handling.

One old and one new coupon were embedded in resin (West System Kinetix R104 Epoxy) in specially designed stainless steel holders (Fig. 2, left). The inner pipe surface of the new coupons and the previously corroded surface of the old coupons were exposed above the resin. The exposed surfaces protruded approximately 10–20 mm above the resin surface.

Aggregate in new concrete samples was dominated by sub-rounded 10 to 15 mm dacitic volcanics and chert with lesser amounts of quartzite, quartz and some rhyolitic volcanics. Aggregate in the old coupons was significantly larger, consisting of 15 to 30 mm rounded andesitic, dacitic and rhyolitic volcanic gravel and cherts with lesser amounts of sandstone, quartzite and quartz. The composition of the new and old coupon cement binder was determined via XRF (Spectro X'Lab 2000) and XRD (Philips X'Pert MPD diffractometer operating at 40 kV, 40 mA) analysis of material chiselled from the centres of the coupons which was subsequently dried overnight at 105 °C before being ground in an agate mill to <53 μm. XRD analysis was performed on the ground material alone and XRF analysis on 40 mm pressed powder tablets to which a small amount of PVA binder had been added. The analyses indicated a similar mineralogical makeup with the exception that the portlandite ($Ca(OH)_2$) component found in the new coupon cement had been replaced by calcite and vaterite (both forms of calcium carbonate) in the old coupons suggesting that most alkaline components of the old coupon material had been completely carbonated over the course of its previous time in service. XRD analysis and microscopic inspection of the pre-existing corrosion layer present on the surface of the old coupons revealed that it principally comprised quartz (most likely from sand particles from the original cement binder retained within the corrosion layer) and gypsum.

2.2. Exposure site

The sewer utilised for the present study is located in Perth (Western Australia). It is part of a sealed sewer system with high H_2S levels. Twenty-four stainless steel holders with concrete coupons were mounted in an inverted position on stainless steel racks fitted in a manhole at the site. In this position the samples were well above the normal 'tidal range' of the wastewater stream and were only immersed at times of high stormwater assisted flow. Thus the coupon faces of interest were unobstructed.

Extensive environmental monitoring was undertaken at the site to determine the diurnal and seasonal variation in environmental conditions in the sewer. Gas temperature, relative humidity and H_2S concentration were logged every 5 min over a 2 week period every 3 months throughout the study period.

2.3. Analyses of recovered coupons

Recovered coupons were left in their stainless steel holders and were inspected initially under a low powered microscope and then examined for changes in surface chemistry/mineralogy. The amount of material lost and depth of the corrosion product layer that had formed were also determined. Details are described below.

2.3.1. Surface pH survey

The surface pH of recovered coupons was examined by using a flat faced pH probe (Extech pH100). A small droplet of deionised, distilled water was placed on the surface of the coupon and allowed to equilibrate for several minutes before the pH of the droplet was measured. Typically 9 individual pH readings were made per coupon. However, for some old coupons and new coupons with advanced corrosion and porous and uneven surface conditions fewer readings were possible although in all cases a minimum of 4 points were measured for each coupon.

Surface pH measurements of new and old control samples kept in a dry, temperature controlled laboratory were also made to assess the extent of background changes in surface pH brought about, for example, by atmospheric carbonation of the samples.

2.3.2. Photogrammetric imaging

The amount of corrosion that took place on the exposed coupon surfaces was determined by using photogrammetry before and after exposure of each coupon, as described below.

Before installation in the sewer, each stainless steel sample holder with coupons was engraved with a unique numerical identifier before being placed in an imaging frame (Fig. 3A). A targeting template comprising 60 unique circular targets (Fig. 3D) was placed in position surrounding the two coupons on the upper rims of the sample container.

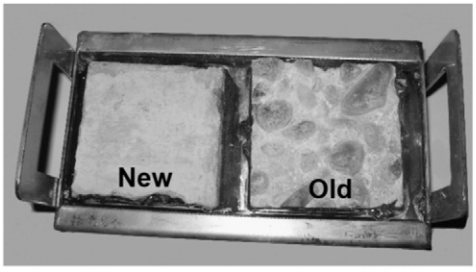

Field coupon sample pair

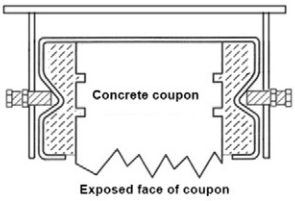

Inverted mounting arrangment

Field samples mounted in the sewer

Fig. 2. Coupon pairs used in field trials (left). Mounting of coupon pairs at the Perth field site (right).

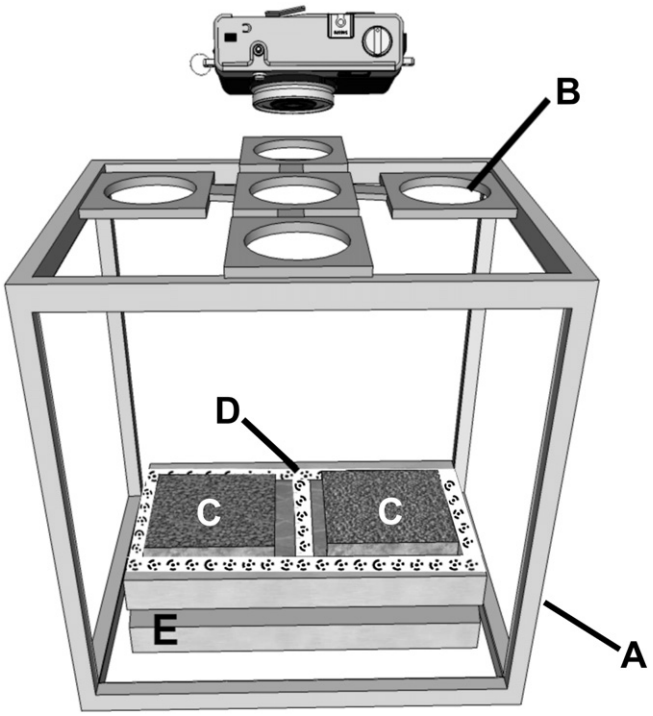

Fig. 3. Setup used to generate photogrammetric 3D images of the coupon surface. A–Imaging frame; B–5 fixed points of view for imaging; C–New and old coupon surfaces; D–Target frame; E–Coupon sample holder.

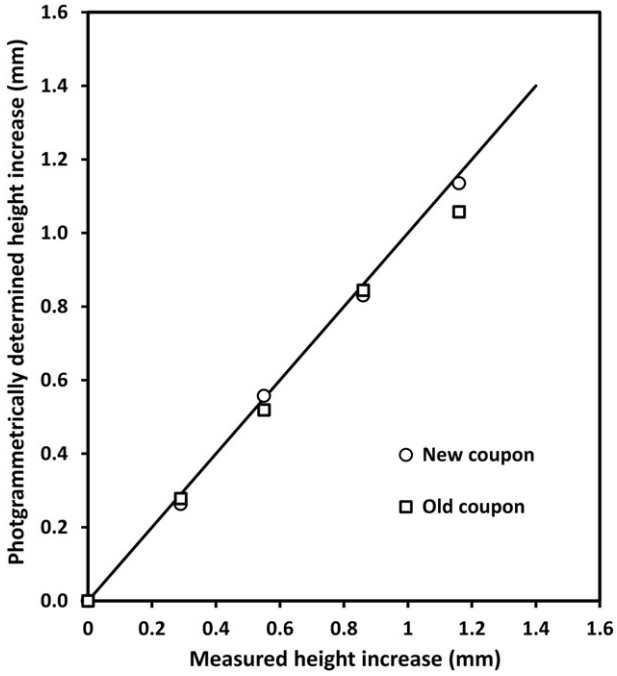

Fig. 5. Results of the sensitivity of the photogrammetric process for determining the average coupon surface height. The solid line represents perfect agreement between measured height increase as determined by digital vernier and heights predicted from the photogrammetry process.

Five images of the exposed surface of each coupon were recorded from the fixed camera positioning rings (Fig. 3B) using a 7.1 megapixel digital camera (focal length 5.99 mm, aperture f/2.6). Subsequently, a photogrammetric imaging software package (PhotoModeler Scanner®) was used to create a 3D cloud point representation of each exposed coupon surface from the series of photographic images. The images are first corrected for lens distortion by using algorithms generated during a camera specific calibration process. The circular targets contained in the target template (which are visible in each image) are then used by the software to: (1) determine the position and orientation of the camera in 3D space at the time each image was taken and (2) scale each image. The plane passing through the targeting template is the reference plane against which the height of the coupon surface is referenced. The information from the five images is then used to generate a unified 3D point cloud representation of the surface of each coupon. The (x,y) grid spacing used to generate the point cloud was set at a nominal 0.5 mm. This typically generated a cloud containing 100,000 to 200,000 points for each coupon surface. An average coupon surface height prior to exposure was then calculated relative to the targeting frame by averaging the z coordinate values.

Upon recovery of the coupons from the sewer the imaging process was repeated for coupons in the 'as-recovered' state i.e. complete with corroded material still present on the coupon surface. The pH survey (see above) then followed immediately. After the pH survey, a high pressure water wash was used to remove the corrosion product and strip the coupons back to 'sound concrete' ('stripped' state). A Karcher 6030MS high pressure water washer delivering water at 8 l/min with a minimum pressure of 20 MPa was used. The nozzle was positioned 300 mm from the coupon surface. A 3 min wash cycle was employed. High pressure water blasting for longer than 3 min did not remove further material. Testing of the washing procedure on new and old control

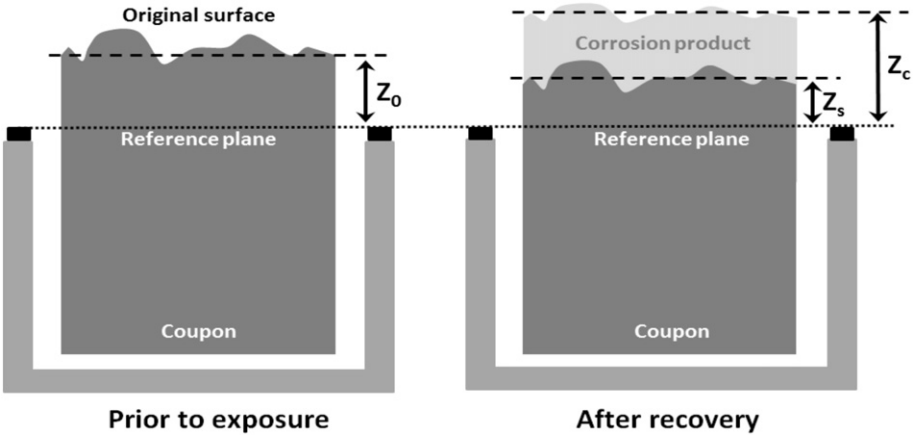

Fig. 4. Determination of corrosion layer depth and concrete losses. Z_0, Z_c, Z_s = the average surface height before exposure, after exposure (with corrosion layer) and after the corrosion layer has been stripped respectively. Corrosion layer depth = $(Z_c - Z_s)$; Corrosion losses = $(Z_0 - Z_s)$.

coupons not placed in the sewer resulted in very minor amounts of material removed from new coupons (an average of 0.04 mm, considered to represent removal of some surface scale). As expected, more material was removed from old concrete coupon control samples (an average 2.05 mm of the existing corrosion layer). These 'background' values were taken into account when calculating the corroded product layer depth and corrosion losses. Following the high pressure water washing a final set of images was taken of the stripped samples.

In each of the sets of 3 images (original, as recovered, and stripped) the target template was used as a fixed reference plane against which the movement of the coupon surface was assessed (upwards as a corrosion product layer accumulates on the surface and down as concrete is corroded away). It is essential that the targeting template is in the same position for each of the three images in a set. To ensure that the targeting template was in the same position for each of the three sets of images great care was taken to ensure that the stainless steel rim of the sample holder, on which the target set sits, was in clean and undamaged condition. No corrosion of the 316 stainless steel rim was observed during the study. In addition, as a further guard against errors resulting from an incorrectly seated target frame, the imaging process was carried out in triplicate at each stage.

After each imaging the 3D surfaces were generated. From these an average surface height relative to the target reference plane was determined for each coupon in the original (Z_0), as-recovered corroded condition (Z_c) and stripped states (Z_s) (Fig. 4). The movement of the 3D surfaces relative to the fixed reference plane was then calculated. From this the depth of the corrosion layer, ($Z_c - Z_s$), and the amount of sound concrete corroded away, ($Z_0 - Z_s$), were determined.

Because of the importance of the amount of corrosion loss in the experimental outcomes, the sensitivity of the photogrammetric process was tested as follows. A coupon holder with a new and old coupon was placed in a target template and the average surface height was determined as before. A piece of thin cardboard was then placed under the coupon holder. The coupons and target frame were re-photographed and the photogrammetry process was used to calculate the new height of the coupon surface relative to the target plane. New pieces of cardboard were added and the process was repeated until the coupons had been raised approximately 1 mm. The change in surface height determined by using the photogrammetric process was then compared to the change in height determined from digital vernier calliper measurements of the cardboard thickness. The results (Fig. 5), show a maximum deviation from the measured values of less than 0.1 mm. This confirms

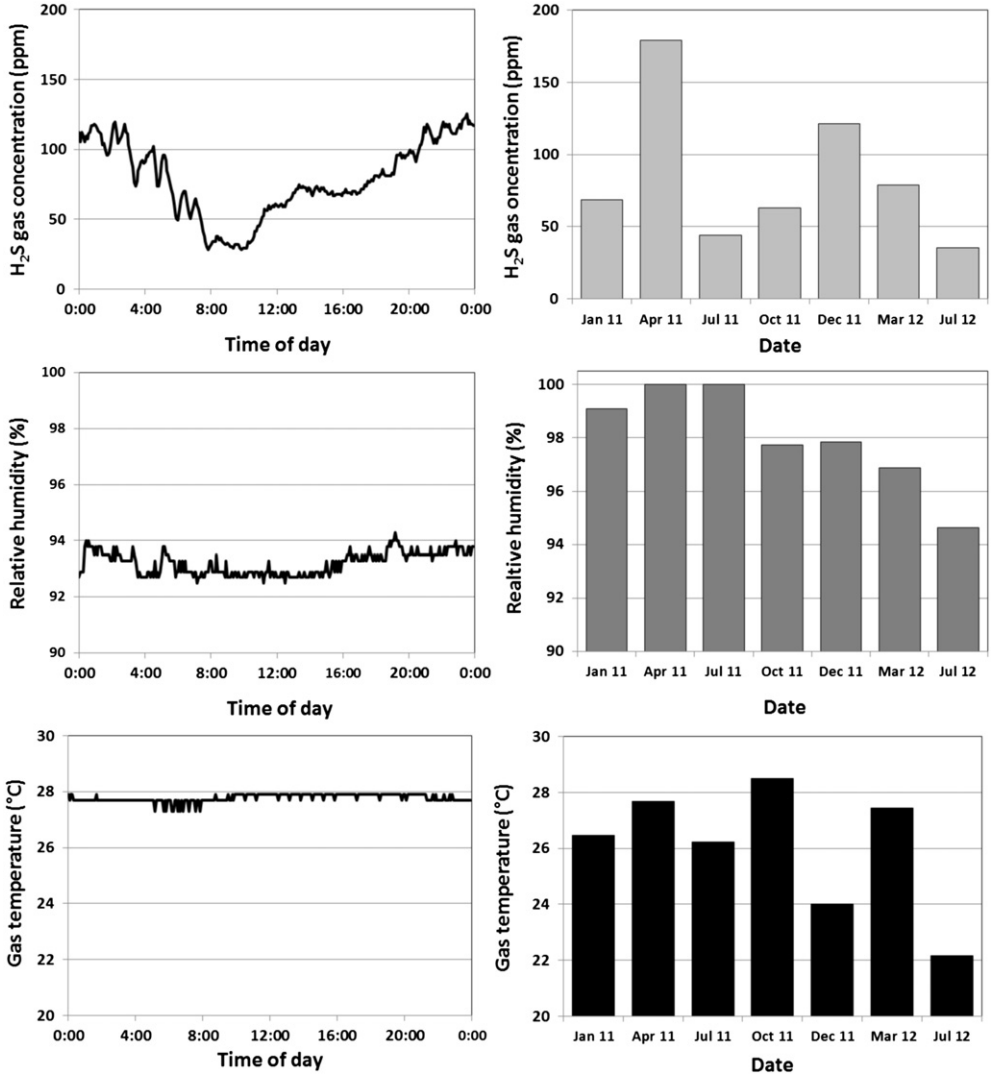

Fig. 6. Diurnal (left) and seasonal variation (right) of H_2S concentration (top), humidity (middle) and gas temperature (bottom) at the Perth sewer site. (The diurnal data shown was recorded on the 24th March 2012).

the accuracy of the photogrammetric process to measure changes in surface movement to 0.1 mm.

3. Experimental results

The field coupons were installed in the sewer during early December 2010. Sets of 3 coupons (3 new and 3 old concretes) were recovered at 7, 14, 19, 26 and 31 months of exposure. All results reported here are the average values for each set of 3 coupons recovered at any one time.

3.1. Environmental conditions

The daily average gas phase H_2S concentration recorded over the study period was 79 ppm; daily average relative humidity was close to saturation (average 98%) and the sewer atmosphere temperatures warm (daily average was 26 °C over the study period). H_2S concentrations in the sewer atmosphere ranged between 7 and 411 ppm, relative humidity between 88 and 100% and temperatures between 22 and 29 °C. On a daily timescale (Fig. 6, left) little variation was generally observed in either relative humidity or gas phase temperature. However, H_2S concentration typically varied considerably throughout the diurnal cycle with concentrations changing by up to 100 ppm over any 24 h period.

Seasonal averages over the study period (Fig. 6, right) also show some variation. H_2S levels were generally highest during the summer/autumnal months with a daily average > 100 ppm reducing to ~40 ppm during winter. Relative humidity has declined over the study period from an average value close to the dew point (>99%) to 94% while the daily average sewer atmosphere temperature ranged from 28.5 °C in October 2011 to a minimum 22.2 °C in July 2012.

3.2. Surface morphology

Changes to the surface morphology were evident on both new and old coupons after 7 months of exposure (Fig. 7). For the new concrete the smooth light grey surface evident prior to exposure was replaced by areas of white crystalline material with pale green and orange areas with an amorphous appearance. In that time the original crystalline corroded surface of the old concrete coupons had been replaced with a soft layer of corrosion product.

After 14 months sufficient corrosion had taken place on the new coupons to expose underlying aggregate. After 26 months of exposure (Fig. 8) the exposed surfaces of both the new and old coupons were essentially indistinguishable. Both surfaces were covered entirely with a soft, highly porous, white corrosion product layer. Inspection of the corroded surfaces under a low powered microscope revealed many cracks and holes, particularly around the exposed aggregate (Fig. 9).

Examination of the recovered coupons under a low power microscope also revealed numerous areas of biological growth on the surfaces of new and old coupons. The growths appeared as small black nodules (~10 μm in diameter) from which emanated pale green/grey branching filamentous structures (hyphae, Fig. 10). Nodules and hyphae were observed on the new coupons retrieved after 7 months of exposure and in increasing numbers after 14 months of exposure. Samples exposed for longer periods however showed fewer numbers.

3.3. Chemistry of recovered coupons

3.3.1. Mineralogy of corrosion product

Previous studies have identified gypsum, ($CaSO_4.2H_2O$) [17,33,40,47], and ettringite, ($3CaO.Al_2O_3.3CaSO_4.31H_2O$) [16,40], as major corrosion products generated in the corrosion of concrete sewer pipe. Major element XRF analysis of coupons in this study revealed that levels of sulfur in the corrosion product were significantly higher in the corrosion product than in the parent concrete for both new and old coupons. XRD analysis confirmed that the major constituent of the corrosion product of both coupon types was gypsum. Ettringite was not found.

3.3.2. Surface pH as a function of exposure time

It has long been recognized that the biotic and abiotic processes operating in sewers lower the surface pH of the concrete over time [13]. The surface pH in turn will influence the type and rate of activity of fungi and bacteria present on the surface and in turn influence the

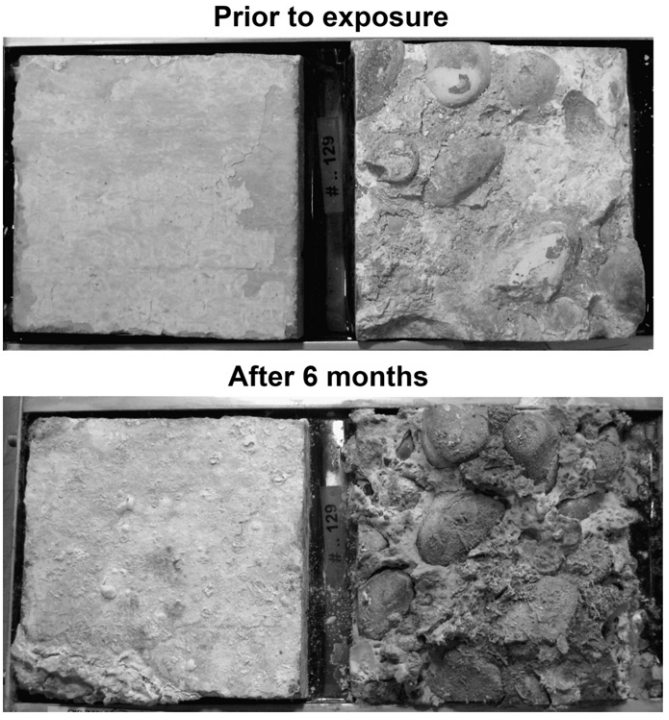

Fig. 7. Changes in surface appearance after 7 months exposure for new coupon (left) and old coupon (right).

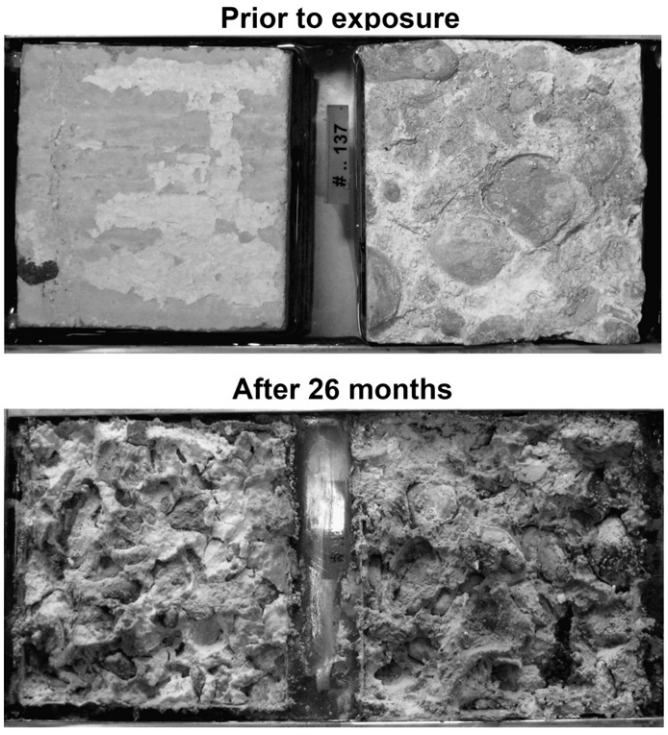

Fig. 8. Changes in surface appearance after 26 months exposure for new coupon (left) and old coupon (right).

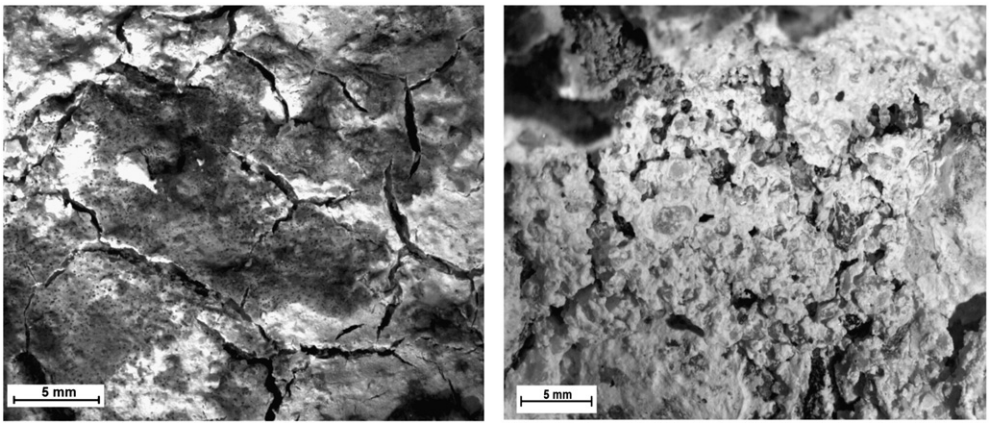

Fig. 9. Cracking and tunnelling of the corroded surface of a new (left) and old coupon (right).

rate of corrosion [16,36]. Thus the rate at which changes in surface pH take place is indicative of the corrosiveness of the sewer atmosphere and the relative activity of bacteria. The surface pH readings obtained for control samples and the new and old concrete coupons as a function of exposure time are shown in Fig. 11.

The surface pH of ~10.1 recorded for new coupons at the commencement of the experiment was significantly below the 11 to 13 normally reported for freshly cast concrete [37]. The initial surface pH declined steadily to an average value of 2.6 after 31 months of exposure (Fig. 11 – left). Over the 31-month period the rate of change of pH was relatively constant for the first 14 months (-0.4 ± 0.03 pH units per month) but slowed thereafter (-0.12 ± 0.03 pH units per month). Over the same period the new concrete control samples declined in surface pH from 10.2 to 9.9.

The old concrete coupons had an average initial surface pH of 8.2 (Fig. 11 – right). This relatively low value compared with new concrete is consistent with their previous exposure history, the presence of an existing layer of corroded product and the carbonation of the portlandite content of the coupon. After 7 months of exposure to the sewer environment the surface pH was approximately 4. Similar values were observed after 14 and 19 months of exposure. After 19 months of exposure the surface pH decreased at a rate of 0.13 pH units per month reaching 2.2 after 31 months exposure. Over the same period the old concrete control samples declined in surface pH from 8.2 to 7.5.

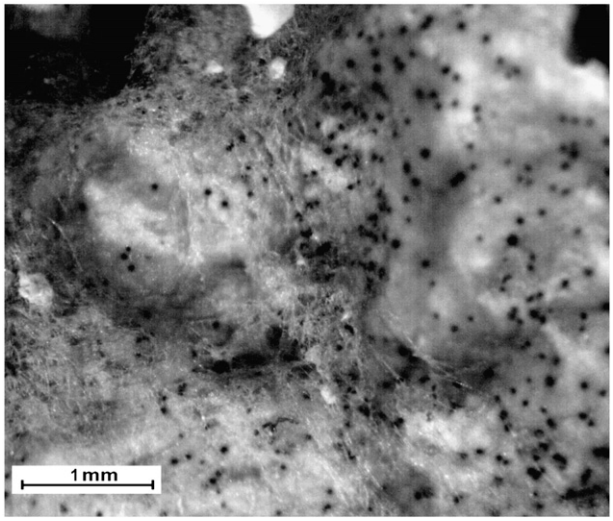

Fig. 10. New coupon surface after 14 months showing nodules and hyphae.

3.4. Corrosion product layer

The average thickness of the corrosion product layer for the new and the old concrete coupons as a function of time is shown in Fig. 12. The build-up of corrosion product on the surface of the new coupon was minimal (<0.5 mm) by the end of the first 7 months. As identified by XRD it consisted of a thin film of small gypsum crystals. At 19 months of exposure the depth of corrosion product had reached approximately 6 mm. By 31 months of exposure the depth was approximately 8.5 mm. By this time the corrosion product layer had taken on a white amorphous appearance with a soft, pasty consistency.

After 7 months of exposure the initial 2 mm thick crystalline corrosion product layer present on the old coupons was replaced with a ~6 mm deep pasty white coating similar in appearance and texture to that present on the new concrete coupons. After 19 months of exposure the depth of corrosion product was approximately 9 mm and by 31 months of exposure was approximately 12 mm.

3.5. Corrosion losses

The loss of sound concrete experienced by the new and old concrete coupons is shown in Fig. 13. After 7 months of exposure the corrosion loss of the new concrete coupons was minimal, averaging 0.2 mm. This increased in a slightly accelerating trend and after 19 and 31 months of exposure the losses were approximately 8.5 mm and 24 mm respectively. Significant losses were also experienced by the old concrete coupons. Losses were apparent from the start and increased linearly with time reaching 28.4 mm after 31 months of exposure.

4. Discussion

As surface conditions on the sewer pipe evolve over time so does the nature, population density and activity of bacterial and fungal communities present on the pipe surface. This was recognized in the three-stage model first proposed by Islander et al. [36] in which concrete sewer pipe corrosion initially proceeds principally by chemical (abiotic) acidification of the pipe surface followed by MIC driven by a succession of evolving microbial communities (Fig. 1). It is therefore appropriate to compare the experimental results of the present study with the stages of a 3-stage model and to ascertain the respective timing of these stages, noting that the environmental conditions were particularly aggressive.

In the present work new concrete coupons were used to examine corrosion behaviour in the early stages of the life of a sewer pipe (stages 1, 2 and possibly the early part of stage 3 in Fig. 1) and old coupons were used to examine the corrosion performance of pipe after corrosion was well advanced (well into stage 3 in Fig. 1). Both the old and the new concretes showed rapid changes and rapid deterioration. After 31 months

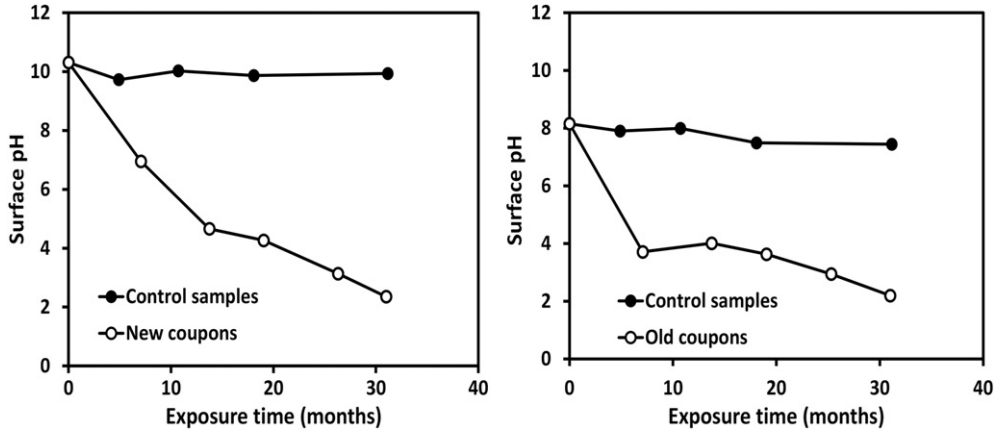

Fig. 11. Surface pH recorded for new coupons (left) and old coupons (right) as a function of time of exposure.

of exposure the surface pH, surface appearance and corrosion rates of the new concrete coupons were almost indistinguishable from those of the old concrete coupons. This indicates that a near-complete picture of the whole corrosion process predicted by the 3-stage model was obtained.

In the 3-stage model, the duration of stages 1 and 2 is delineated by the time taken for the surface pH to drop to 9 and 4 respectively. For the new concrete the surface pH was 10.2 immediately prior to installation in the sewer (Fig. 11 – left). This pH reading is not that for the bulk concrete which typically is much higher (around 13 to 14). This is a matter for further investigation but at this stage it is speculated that carbonation by atmospheric CO_2 may have been involved in the time between pipe manufacture and the surface pH measurement on coupons (approximately 6 months). Normally carbonation is considered to be a very slow process, but this is based primarily on the rate at which the bulk concrete rather than the surface is carbonated. Irrespective of the precise reason, the lower than expected surface pH has some influence on the subsequent development of the surface pH, the chemical reactions and the nature of surface biological activity.

The surface pH of 10.2 declined rapidly once the new concrete coupons were exposed to the sewer atmosphere (Fig. 11 – left). As noted this resulted in the surfaces reaching pH = 9 and thus the transition from stages 1 to 2 occurred within 3 months. In previous studies Okabe et al. [8] and Roberts et al. [43] have also observed relatively short stage 1 intervals (56 days at $H_2S = 30 \pm 20$ ppm and 60–90 days at $H_2S = 50$ ppm respectively). Also fungal colonies were observed on the coupon surfaces at 7 months of exposure indicating that, by this time, surface conditions had changed sufficiently so as to be supportive of microbiological activity. The transition to stage 3 (pH = 4) was reached at 21 months of exposure. Hence for the new concrete the duration of stage 2 is about 18 months.

For the old concrete, the transition through to stage 3 was much faster, taking less than 7 months for the surfaces to come to equilibrium with the sewer environment and for surface pH to decline to pH = 3 to 4. This places these coupons well within stage 3 after 7 months of exposure (Fig. 11 – right). This suggests that the results for the old concrete coupons after 7 months can be taken as indicative of corrosion behaviour for long exposures.

It is now possible to compare these transition times to both the corrosion losses and the depth of the corrosion product layer, using the results for the new concrete to represent the early exposure period and the old concrete the later exposure period (Fig. 14). For the new concrete (left) there is minimal loss of concrete (<0.2 mm) during the abiotic corrosion phase 1 and also, in consequence, minimal depth of corrosion product. Corrosion losses remained minimal for several months into stage 2 before then increasing quickly to reach an approximately constant rate of 9 mm/year. The reason for the delay is not obvious and warrants investigation.

When the new concrete deterioration reaches stage 3, there is a slight increase in the rate of corrosion to about 12 mm/year at 31 months of exposure. This may be the result of the surface pH having decreased to around 4, thus allowing acidophilic bacteria to begin to succeed the neutrophilic bacteria.

For the old concrete (Fig. 14, right) the data trend in stage 3 is linear, consistent with the rate observed for the new concrete coupons at 31 months. Linear regression shows that the corrosion rate is 11 mm/year ($r^2 = 0.99$).

Fig. 12. Development of the corrosion layer as a function of exposure time. Each data point is the average height change of 3 coupons and the error bars are the standard deviation of the 3 measurements.

Fig. 13. Losses experienced by new coupons and old coupons as a function of exposure time. Each data point is the average height change of 3 coupons and the error bars are the standard deviation of the 3 measurements.

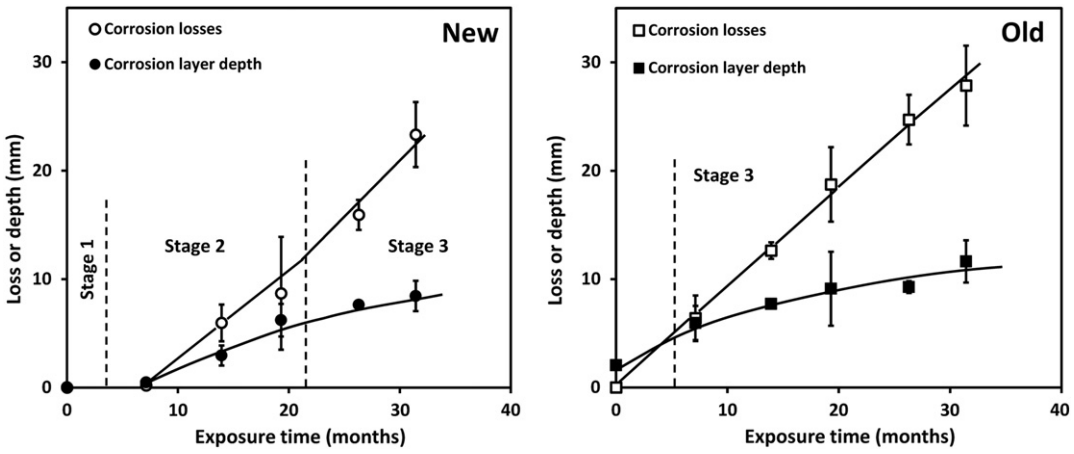

Fig. 14. Corrosion losses and corrosion layer depth observed with stage timings superimposed for new coupons (left) and old coupons (right).

For both the new and the old concretes the constant value of the corrosion rates in stages 2 and 3 suggests that the increasing thickness and volume of the corrosion products formed has little influence on the rate of corrosion. If the corrosion products impeded oxygen diffusion or the transport of nutrients and/or acid, a declining rate of corrosion would have occurred. This lack of influence of the corrosion product is considered the direct result of the soft and cracked nature of the corrosion product (see Fig. 9).

The results of the above analysis can be plotted in terms of corrosion rate as a function of time (Fig. 15). Although these results are for the aggressive corrosion site considered in the present paper, they are consistent entirely with the 3-stage model for corrosion loss proposed by Islander et al. [36]. This indicates the validity of using the corrosion results from the aggressive corrosion conditions described in the present paper.

For practical purposes a more useful representation of the corrosion of concrete sewers is the progression of corrosion loss with time. The sharp change from almost no corrosion in the early exposure period to an essentially steady-state condition for longer term exposures (Fig. 15) means that the corrosion loss function may be considered as essentially bilinear (Fig. 16). Further, in view of the consistency with the model by Islander et al. [36] this can be expected to be the case also for corrosion in conditions less aggressive than those considered in the present paper.

The bilinear model can be parameterised by using just two parameters – the time t_i for corrosion to initiate and the longer-term steady-state corrosion rate r (Fig. 16). For the data considered herein the values are $t_i = 0.9$ years and $r = 12$ mm/year. More generally, the values of these parameters will need to be estimated from data for other sewer internal environmental and operational conditions. It should be clear, however, that with lower temperatures and less aggressive conditions it can be expected that t_i will be greater and r lower than these values. The precise relationships between the parameters t_i and r and the influencing factors including temperature, relative humidity and hydrogen sulfide levels remain a matter for further research. This work is currently underway and will be reported in due course.

Finally, Fig. 16 can be used to provide a simple example of the prediction of the service life of a standard reinforced concrete sewer pipe with, for example, an initial 100 mm depth of concrete cover separating the metal reinforcing structure from the sewer atmosphere. For the internal sewer environment described herein, Fig. 16 shows that it would take 9.2 years for cover concrete to be corroded away exposing the metal reinforcing at which point it is assumed that the pipe has reached the end of its service life. Similar calculations can be made for differing levels of concrete cover.

5. Conclusion

The results of the present study of the corrosion of new and 70 year old concrete exposed to a realistic but particularly aggressive sewer environment show that new concrete passes through 3 stages, characterized by decreasing surface alkalinity and the eventual development of long-term steady-state corrosion. Despite the severity of the exposure

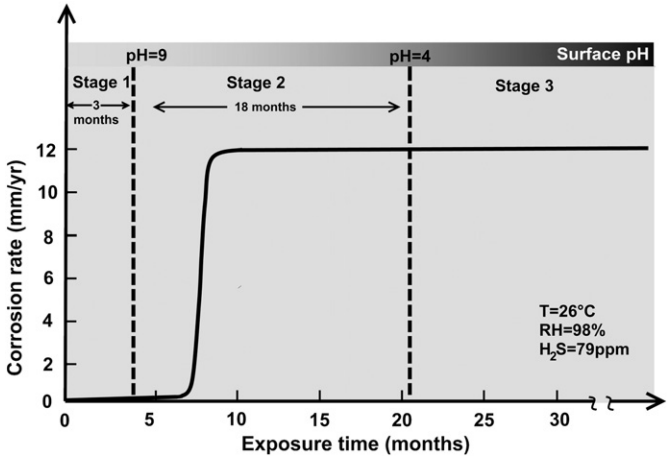

Fig. 15. A quantitative representation of the three stages of corrosion of concrete pipe for exposure conditions at the Perth sewer site.

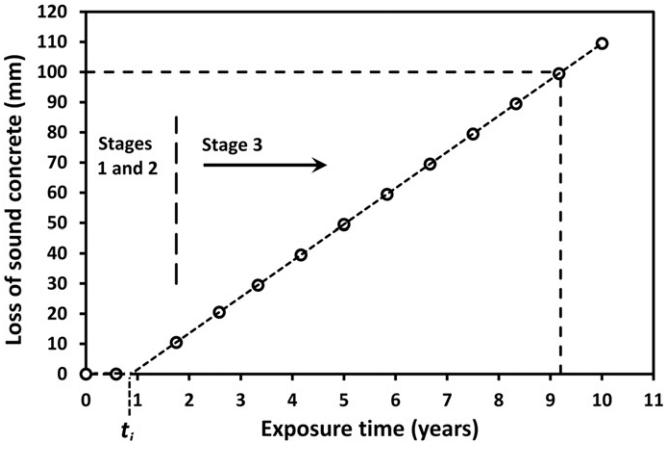

Fig. 16. Predicted corrosion losses for an unprotected concrete sewer pipe under the environmental conditions considered herein. For a pipe with initial concrete cover depth of 100 mm a service life of 9.2 years is predicted. Data is fitted with a simple bilinear model (see text).

conditions, these stages are consistent with the model proposed earlier by Islander et al. [36] for the changing corrosion rate of concrete sewers under typical exposure conditions. The older concretes showed corrosion behaviour consistent with stage 3 of the model. The results can be simplified to a bilinear model for corrosion loss, with negligible corrosion in the early period and corrosion at a constant rate after initiation. The data from the present study provide one set of parameters for the bilinear model but further field data is required to calibrate the to less severe sewer environments.

Acknowledgements

The authors acknowledge the financial support of the Australian Research Council (through ARC Linkage Project LP0882016) and Industry Partners Barwon Regional Water Corporation, CH2M Hill, Gold Coast Water, Hunter Water Corporation, Melbourne Water Corporation, South Australia Water, South East Water Limited, Sydney Water Corporation, United Water International, Water Quality Research Australia and Western Australia Water Corporation, all partners in the Sewer Corrosion and Odour Research (SCORe) Project (www.score.org.au) that also includes the University of Queensland, University of Sydney and University of Technology Sydney. A special thanks also to Professor Stephen Fityus for his help in specifying the lithology of the coupon aggregates.

References

[1] US Environmental Protection Agency, Hydrogen Sulfide Corrosion in Wastewater Collection and Treatment Systems: Report to Congress. Technical report, 430/09-91-010, 1991.
[2] J. Vollertsen, A.H. Nielsen, H.S. Jensen, E.A. Rudelle, T. Hvitved-Jacobsen, Modeling the corrosion of concrete sewers, 12th International Conference on Urban Drainage, Porto Alegre/Brazil, 2011.
[3] R.E. Melchers, Corrosion uncertainty modelling for steel structures, J. Constr. Steel Res. 52 (1999) 3–19.
[4] R.E. Melchers, P.A. Wells, Modelling the long term corrosion of reinforced concrete sewers, 7th IWA Leading-Edge Conference on Water and Wastewater Technologies, Phoenix, Arizona, USA, 2–4 June 2010, 2009.
[5] P.A. Wells, R.E. Melchers, Factors involved in the long term corrosion of concrete sewers (Paper 54), Conference Proceedings Corrosion and Prevention 2009: The Management of Infrastructure Deterioration, Coffs Harbour, Australia, 2009.
[6] R.E. Melchers, R. Jeffrey, Influence of water velocity on marine immersion corrosion of mild steel, Corrosion 60 (2004) 84–94.
[7] B.J. Little, J.S. Lee, R.I. Ray, The influence of marine biofilms on corrosion: a concise review, Electrochim. Acta 54 (2008) 2–7.
[8] S. Okabe, M. Odagiri, T. Ito, H. Satoh, Succession of sulfur-oxidizing bacteria in the microbial community on corroding concrete in sewer systems, Appl. Environ. Microbiol. 73 (2007) 971–980.
[9] W.M. Olmstead, H. Hamlin, Converting portions of the Los Angeles outfall sewer into a septic tank, Eng. News 44 (19) (1900) 317–318.
[10] R. Pomeroy, F.D. Bowlus, Progress report on sulfide control research, Sewage Works J. 18 (1946) 597–640.
[11] C.D. Parker, The corrosion of concrete 1. The isolation of a species of bacterium associated with the corrosion of concrete exposed to atmospheres containing hydrogen sulphides, Aust. J. Exp. Biol. Med. Sci. 23 (1945) 81–90.
[12] C.D. Parker, The corrosion of concrete 2. The function of *Thiobacillus concretivorus* (nov. spec.) in the corrosion of concrete exposed to atmospheres containing hydrogen sulphides, Aust. J. Exp. Biol. Med. Sci. 23 (1945) 91–98.
[13] C.D. Parker, Mechanics of corrosion of concrete sewers by hydrogen sulfide, Sewage Ind. Waste. 23 (1951) 1477–1485.
[14] D. Nica, J.L. Davis, L. Kirby, G. Zuo, D.J. Roberts, Isolation and characterization of microorganisms involved in the biodeterioration of concrete in sewers, Int. Biodeterior. Biodegrad. 46 (2000) 61–68.
[15] K.S. Cho, T. Mori, A newly isolated fungus participates in the corrosion of concrete sewer pipes, Water Sci. Technol. 31 (1995) 263–271.
[16] J.L. Davis, D. Nica, K. Shields, D.J. Roberts, Analysis of concrete from corroded sewer pipe, Int. Biodeterior. Biodegrad. 42 (1998) 75–84.
[17] W. Sand, E. Bock, Concrete corrosion in the Hamburg Sewer system, Environ. Technol. Lett. 5 (1984) 517–528.
[18] B.I. Cayford, P.G. Dennis, J. Keller, G.W. Tyson, P.L. Bond, High-throughput amplicon sequencing reveals distinct communities within a corroding concrete sewer system, Appl. Environ. Microbiol. 78 (2012) 7160–7162.
[19] B.I. Cayford, G.W. Tyson, J. Keller, P.L. Bond, Microbial community composition of biofilms associated with sewer corrosion, 6th International Conference on Sewer Processes and Networks November 7–10, 2010, Surfers Paradise, Gold Coast, Australia, 2010.
[20] K.B. Tator, Preventing hydrogen sulfide and microbially influenced corrosion in wastewater facilities, Mater. Perform. 42 (2003) 32–37.
[21] J.D. Gu, T.E. Ford, N.S. Berke, R. Mitchell, Biodeterioration of concrete by the fungus *Fusarium*, Int. Biodeterior. Biodegrad. 41 (1998) 101–109.
[22] R.L. Morton, W.A. Yanko, D.W. Graham, R.G. Arnold, Relationships between metal concentrations and crown corrosion in Los Angeles County sewers, Res. J. Water Pollut. Control Fed. 63 (1991) 789–798.
[23] W. Sand, T. Dumas, S. Marcdargent, Tests for biogenic sulfuric acid corrosion in a simulation chamber confirm the on-site performance of calcium aluminate-based concretes in sewage applications, in: K.D. Basham (Ed.), Infrastructure: New Materials and Methods of Repair — Proceedings of the Third Materials Engineering Conference, ASCE, New York, NY, 1992, pp. 35–55.
[24] K. Milde, W. Sand, W. Wolff, E. Bock, Thiobacilli of the corroded concrete walls of the Hamburg sewer system, J. Gen. Microbiol. 129 (1983) 1327–1333.
[25] W. Sand, Importance of hydrogen sulfide, thiosulfate, and methylmercaptan for growth of thiobacilli during simulation of concrete corrosion, Appl. Environ. Microbiol. 53 (1987) 1645–1648.
[26] U.S. EPA, Process Design Manual for Sulfide Control in Sanitary Sewerage Systems, US EPA, 625/1-74-005, Technology Transfer, Washington DC, 1974.
[27] D.K.B. Thistlethwayte, The control of sulphides in sewerage systems, Butterworths Pty Ltd., Sydney Australia, 1972.
[28] H.S. Jensen, Hydrogen sulfide induced concrete corrosion of sewer networks, Section of Environmental Engineering, Aalborg University, 2009, p. 67.
[29] H.S. Jensen, A.H. Nielsen, T. Hvitved-Jacobsen, J. Vollertsen, Modeling of hydrogen sulfide oxidation in concrete corrosion products from sewer pipes, Water Environ. Res. 81 (2009) 365–373.
[30] H.S. Jensen, A.H. Nielsen, P.N.L. Lens, T. Hvitved-Jacobsen, J. Vollertsen, Hydrogen sulphide removal from corroding concrete: comparison between surface removal rates and biomass activity, Environ. Technol. 30 (2009) 1291–1296.
[31] J. Vollertsen, A.H. Nielsen, H.S. Jensen, T. Wium-Andersen, T. Hvitved-Jacobsen, Corrosion of concrete sewers — The kinetics of hydrogen sulfide oxidation, Sci. Total Environ. 394 (2008) 162–170.
[32] A.P. Joseph, J. Keller, H. Bustamante, P.L. Bond, Surface neutralization and H_2S oxidation at early stages of sewer corrosion: influence of temperature, relative humidity and H_2S concentration, Water Res. 46 (2012) 4235–4245.
[33] A. Bielefeldt, M.G.D. Gutierrez-Padilla, S. Ovtchinnikov, J. Silverstein, M. Hernandez, Bacterial kinetics of sulfur oxidizing bacteria and their biodeterioration rates of concrete sewer pipe samples, J. Environ. Eng. 136 (2010) 731–738.
[34] H.S. Jensen, P.N.L. Lens, J.L. Nielsen, K. Bester, A.H. Nielsen, T. Hvitved-Jacobsen, J. Vollertsen, Growth kinetics of hydrogen sulfide oxidizing bacteria in corroded concrete from sewers, J. Hazard. Mater. 189 (2011) 685–691.
[35] H. Satoh, M. Odagiri, T. Ito, S. Okabe, Microbial community structures and in situ sulfate-reducing and sulfur-oxidizing activities in biofilms developed on mortar specimens in a corroded sewer system, Water Res. 43 (2009) 4729–4739.
[36] R.L. Islander, J.S. Devinny, F. Mansfeld, A. Postyn, S. Hong, Microbial ecology of crown corrosion in sewers, J. Environ. Eng. ASCE 117 (1991) 751–770.
[37] F.M. Lea, The Chemistry of Cement and Concrete, 3rd edition Edward Arnold Ltd., London, 1970.
[38] M. Diercks, W. Sand, E. Bock, Microbial corrosion of concrete, Experientia 47 (1991) 514–516.
[39] W. Sand, B. Ahlers, E. Bock, The impact of microorganisms, especially nitric acid producing bacteria, on the deterioration of natural stones, Science, Technology, and European Cultural Heritage: Proceedings of the European symposium Bologna, Italy 13–16 June 1989, 1991, pp. 481–484.
[40] T. Mori, T. Nonaka, K. Tazaki, M. Koga, Y. Hikosaka, S. Noda, Interactions of nutrients, moisture and pH on microbial corrosion of concrete sewer pipes, Water Res. 26 (1992) 29–37.
[41] M. Valix, D. Zamri, H. Mineyama, W.H. Cheung, J. Shi, H. Bustamante, Microbiologically induced corrosion of concrete and protective coatings in gravity sewers, Chin. J. Chem. Eng. 20 (2012) 433–438.
[42] A.K. Parande, P.L. Ramsamy, S. Ethirajan, C.R.K. Rao, N. Palamisamy, Deterioration of reinforced concrete in sewer environments, Proc. Inst. Civ. Eng. - Munic. Eng. 159 (2006) 11–20.
[43] D.J. Roberts, D. Nica, G. Zuo, J.L. Davis, Quantifying microbially induced deterioration of concrete: initial studies, Int. Biodeterior. Biodegrad. 49 (2002) 227–234.
[44] E. Vincke, N. Boon, W. Verstraete, Analysis of the microbial communities on corroded concrete sewer pipes — a case study, Appl. Microbiol. Biotechnol. 57 (2001) 776–785.
[45] M. Hernandez, E.A. Marchand, D. Roberts, J. Peccia, In situ assessment of active *Thiobacillus* species in corroding concrete sewers using fluorescent RNA probes, Int. Biodeterior. Biodegrad. 49 (2002) 271–276.
[46] R. Rootsey, Z. Yuan, The Sewer Corrosion and Odour Research (SCORE) project, Water, March 2011, pp. 57–61.
[47] I. Fernandes, M. Pericão, P. Hagelia, F. Noronha, M. Ribeiro, J. Maia, Identification of acid attack on concrete of a sewage system, Mater. Struct. 45 (2012) 337–350